Environ. Sci. Technol. **2005**, *39,* 1378−1383

Cytotoxicity of Carbon Nanomaterials: Single-Wall Nanotube, Multi-Wall Nanotube, and Fullerene

GUANG JIA,[†,‡] HAIFANG WANG,[§] LEI YAN,[†] XIANG WANG,[†] RONGJUAN PEI,[†] TAO YAN,[†] YULIANG ZHAO,*[,‡,§] AND XINBIAO GUO*[,†]

Department of Occupational and Environmental Health, School of Public Health, Peking University, Beijing 100083, China, Laboratory for Bio-Environmental Health Sciences of Nanoscale Materials, Institute of High Energy Physics, Chinese Academy of Sciences, Beijing 100049, China, and College of Chemistry and Molecular Engineering, Peking University, Beijing 100871, China

A cytotoxicity test protocol for single-wall nanotubes (SWNTs), multi-wall nanotubes (with diameters ranging from 10 to 20 nm, MWNT10), and fullerene (C_{60}) was tested. Profound cytotoxicity of SWNTs was observed in alveolar macrophage (AM) after a 6-h exposure in vitro. The cytotoxicity increases by as high as ∼35% when the dosage of SWNTs was increased by 11.30 μg/cm^2. No significant toxicity was observed for C_{60} up to a dose of 226.00 μg/cm^2. The cytotoxicity apparently follows a sequence order on a mass basis: SWNTs > MWNT10 > quartz > C_{60}. SWNTs significantly impaired phagocytosis of AM at the low dose of 0.38 μg/cm^2, whereas MWNT10 and C_{60} induced injury only at the high dose of 3.06 μg/cm^2. The macrophages exposed to SWNTs or MWNT10 of 3.06 μg/cm^2 showed characteristic features of necrosis and degeneration. A sign of apoptotic cell death likely existed. Carbon nanomaterials with different geometric structures exhibit quite different cytotoxicity and bioactivity in vitro, although they may not be accurately reflected in the comparative toxicity in vivo.

Introduction

Because of the unique physical and chemical characteristics, nanosized materials and nanoscale technologies are changing many basic scientific concepts. With increasing industrial productions of nanomaterial, public concern on their environmental and health effects is growing rapidly. To date, little is known about how nanosized materials behave in the environment and in the human body. Current studies on the toxicological and environmental effects of nanomaterial are still scarce (*1*). This has led to a serious public debate on the necessity for a ban or moratorium on the research, development, and sale of nanomaterials and nanoscale products (*1*).

One of the most widely studied and used namaterials is carbon nanomaterial. For example, fullerene, endohedral fullerene (fullerene cage encapsulating atoms, clusters, or small molecules) and carbon nanotube (including single-wall nanotubes, SWNTs; and multiwall nanotubes, MWNTs) (*2*) have been proposed for many potential applications such as superconductor material, optical devices, molecular switch (memory switch), high-temperature superconductive material, quantum computer, and biomedical use. It has been predicted that tens or even hundreds of tons of carbon nanomaterials will be produced worldwide every year (*3*). That will undoubtedly increase the risk of human and environmental exposures to the carbon nanomaterials (*4, 5*).

Recently, Warheit et al. studied the pulmonary toxicity of SWNTs in rats and found the incidence of a non-dose-dependent series of multifocal granulomas (*6*). Similar work on the pulmonary toxicity of SWNTs in mice has been reported by Lam et al. (*7*). It was found that SWNTs induced dose-dependent interstitial granulomas and, in pulmonary injuries, a carbon nanotube was much more toxic than quartz.

As enlightened by these studies, we conducted the cytotoxicity study of the carbon nanomaterials with AM (alveolar macrophage), which constitute the first line of immunological defense against the invading particles in the lung. So far, the reported data are not sufficient to ascertain the impact of carbon nanomaterials on the environment and human health (*8*). In this work, SWNTs, MWNTs (with a diameter of 10−20 nm, MWNT10), and fullerenes (C_{60}) were chosen because of their definite nanostructures, different size distributions, different surface areas, and diverse physical and chemical properties. These nanomaterials are all made of carbon atoms but with distinct geometries. They provide an opportunity to explore the comparative toxicity particularly originated by geometrical structure and physical properties. As is well-known, the pathogenicity of inhaled particles largely depends on their geometry (*9*). The objectives of this study were to determine the cytotoxicity to AM caused by the above-mentioned carbon nanomaterials in vitro and to compare the responses of AM when exposed to various carbon nanomaterials.

To this end, three basic approaches were selected and tested. (i) Assay on the inhibition of the mitochondrial dehydrogenase activity. This is a well-known method commonly used in the cytotoxicity studies. (ii) Phagocytic response to latex beads. This can be used as an indicator, demonstrating the immunological function of AM. (iii) Electron transmission microscopic (TEM) analysis, which provides direct visual observation on the ultrastructural alterations of the impaired AM. Quartz (SiO_2), a serious occupational health hazard in chronic inhalation exposure, was used as a control.

Materials and Methods

Materials. SWNTs have a diameter of ca. 1.4 nm and a mean length of ca. 1 μm (with a wide length distribution ranging from tens of nanometers to several micrometers, as determined by TEM). The product, made by the electric arc discharge method, was obtained from Prof. Gu Zhen-Nan of Peking University (Beijing, China) (*10*). SWNTs were purified to a purity of ∼90% according to method of Gu and coworkers (*11*). The main impurity in the SWNTs sample was amorphous carbon. The catalysts (Fe, Y, and Ni) that remained in the sample were determined in trace amounts by both X-ray photoelectron spectroscopic (XPS) and X-ray fluorenscence (XRF) analyses. MWNT10 made by the chemical vaporization deposition (CVD) method was obtained from Shenzhen Nanotech Port Co. Ltd. The MWNT10 was 10−20

* Authors to whom correspondence should be addressed. Fax: +86-10-88233191 (Y.Z.); +86-10-62015583 (G.X.). E-mail: zhaoyuliang@ihep.ac.cn (Y.Z.); xguo@bjmu.edu.cn (G.X.).
† School of Public Health, Peking University.
‡ Chinese Academy of Sciences.
§ College of Chemistry and Molecular Engineering, Peking University.

10.1021/es048729l CCC: $30.25

Published on Web 01/07/2005

nm in diameter and 0.5−40 μm in length with a specific surface area 40−300 m^2/g according to BET analysis. Purity was great than 95%, containing <3% amorphous carbon determined by thermal gravity analysis and ca. 0.6% Ni analyzed by EDS and XRF. C_{60} made by the electric arc discharge method was obtained also from Prof. Gu's lab and purified to >99.9% by the HPLC method. The number of C_{60} was $8.36 \times 10^{14}/\mu g$. But for the nanotubes, it is inadequate to express a dose in the number of particles because they are tubes with a wide length distribution and likely behave differently than molecules. The surface area of a nanotube varies with the degree of aggregation of nanotubes. The doses used in the experiment for SWNTs and C_{60} were 0, 1.41, 2.82, 5.65, 11.30, 28.20, 56.50, 113.00, and 226.00 $\mu g/cm^2$, respectively; for MWNT10, they were 0, 1.41, 2.82, 5.65, 11.30, and 22.60 $\mu g/cm^2$, respectively. Quartz with well-documented biological activity was used as a control. It was obtained from the National Institute for Occupational Health and Poison Control, Chinese Center for Disease Control and Prevention (Beijing, China) with a purity of 99%. More than 95% of the crystalline silica particles were less than 5 μm in diameter. The surface area for a crystalline silica particle was estimated to be around 78.5 μm^2.

RPMI 1640 medium (without L-glutamine and phenol red) was purchased from Hyclone (Logan, UT); fetal bovine serum (FBS) and Dulbecco's balanced phosphate-buffered saline (PBS^-) without calcium and magnesium salts were obtained from Gibco BRL (Paisley, UK). 3-(4,5-Dimethylthiazol-2-y1)−2,5-diphenyl tetrazoliumbromide (MTT) was purchased from Sino-American Biotec, and latex fluorescent beads (2 μm) were from Sigma Chemicals Company (Poole, Dorset, UK).

Preparation of Carbon Particle Suspension. Particles were freshly suspended in culture medium (RPMI 1640 medium supplemented with 10% FBS) with a Dounce homogenizer (about 20 strokes) and sonicated for 20 min in a short break every 2 min for vortexing on ice. A stable suspension of carbon particles was obtained in this way and used immediately.

The 10−100 SWNTs usually form rather tight aggregates. About 4−6 MWNTs aggregate into one thin bundle. In the present experiment, no dispersing reagent (such as surfactant SDS) was used to break the as-prepared nanotube bundles. Therefore, the cytotoxicity test was likely limited to AM caused by exposure to the nanotube bundles. If a dispersing reagent was used, the intrinsic property of nanotube would be substantially altered. The dispersed system could differ far from the case of the exposure to the pure nanotube bundles.

Isolation of Alveolar Macrophages. Adult pathogen-free healthy guinea pigs (250−300 g) were purchased from Laboratory Animal Center of Peking University. AM was isolated by bronchi alveolar lavage (BAL) (*12*). The lung was lavaged 5 times by intratracheal instillation using 10 mL of calcium magnesium-free PBS. AM isolated from collected lung lavage fluid by centrifugation at 800 rpm for 8 min was then re-suspended in RPMI 1640 medium containing 10% FBS. Average yield was $6 \times 10^6 - 10 \times 10^6$ cells per guinea pig, of which more than 90% were viable by Wright's staining. The macrophages were plated at a density of 2×10^5/mL viable cells per well in Costar 24 multi-well plates or culture dishes with 5 cm diameter and allowed to attach to the plastic matrix for 2 h at 37 °C. After removing the medium and non-adherent cells, the fresh cell monolayer was exposed to the prepared nanomaterial suspensions of tested nanomaterial in culture medium for different experiments. Co-cultured systems (macrophage-epithelial cell) were not used in this study.

Assessment of Cytotoxicity. The cytotoxicity induced by the tested nanomaterial was determined by the MTT reduction experiment. MTT assay is based on the mitochondrial dehydrogenase activities (*13*). Briefly, after exposing AM to nanomaterial for 3 h, MTT (20 μl, 5 mg/mL of PBS) was added to each AM sample and incubated for another 3 h. Supernatants were removed, and the formed dark blue formazan crystals were dissolved with 1 mL of 1 N HCl−2-propanol (1:24, v/v). The samples were left at room temperature for 10 min and then centrifuged at 900*g* for 15 min at 18 °C to remove any particles present in the supernatant. The supernatants were re-aliquoted into wells (200 μL/well) of a new 96-well plate, and their absorbance was recorded at 570 nm in a Biorad Microplate Reader. The relative cytotoxicity was expressed as percentage of $[OD_{control} - OD_{particle}]/OD_{control}$. Each experiment was performed at least in triplicate.

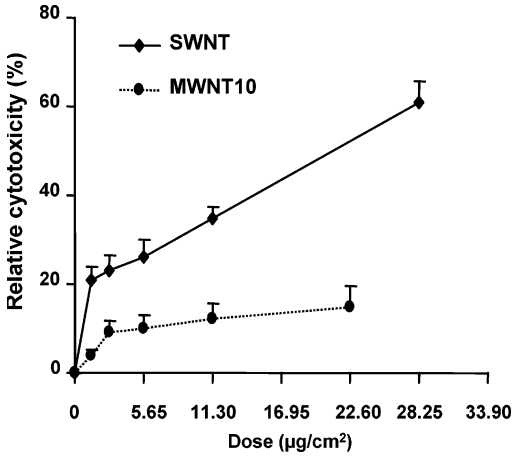

FIGURE 1. Dose-dependent cytotoxicity in AM exposed to SWNTs and MWNT10 for 6 h. Results are mean ± SE of the triplicate experiments, $P < 0.05$. The cytotoxicity was determined by MTT reduction method.

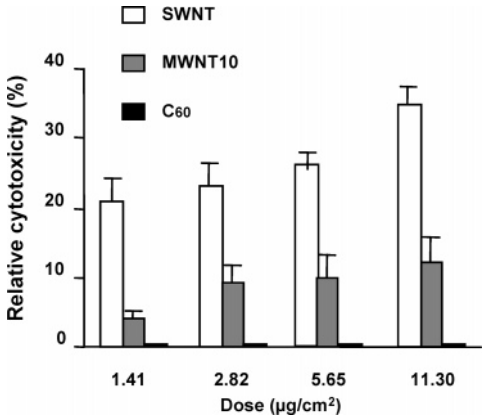

FIGURE 2. Comparison with cytotoxicity to AM among SWNTs, MWNT10, and C_{60} at different dosage. Results are mean ± SE of triplicate experiments, $P < 0.05$.

Phagocytic Response of AM to Latex Beads. The phagocytic ability of the isolated primary AM after 6-h exposure to carbon nanomaterial was assessed by measuring their ability to phagocytose 2 μm colloid gold latex beads. After 6-h exposure to various doses of the tested nanomaterial, AM were transferred to a fresh 1640 medium containing 2 μm latex beads at a bead-to-macrophage ratio of 10:1 for approximately 16 h (*12*). The controls were treated as the test samples just without the tested particles. Beads not phagocytosed were removed partly by discarding the culture medium and washing the cells with PBS for two times. The cells were observed under a fluorescent microscope (NikonTE2000-S), which permits examination with both visible and UV fluorescence light. We can distinguish adhered particles and internalized (phagocytized) particles by finely adjusting the focal length in the microscopic observation.

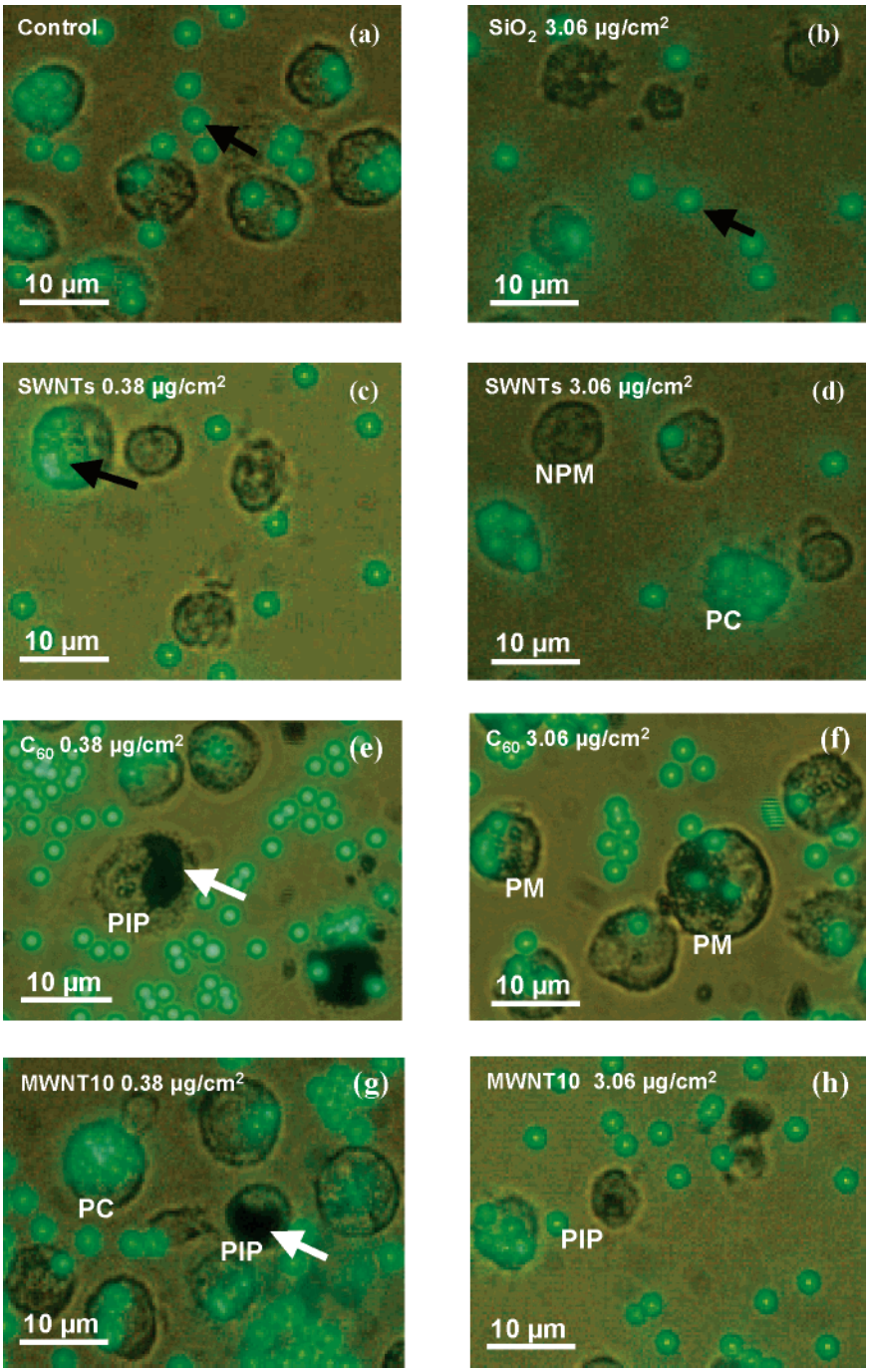

FIGURE 3. Representative images of AM exposed to SWNTs, MWNT10, and C_{60}. The white arrows point to carbon nanoparticles, and the black arrows indicate latex beads. Four types of cells were observed (for detail, see the text) and marked by PM (phagocytic macrophage), PIP (AM phagocytosis inhibited by particles), NPM (nonphagocytic macrophages), and PC (AM phagocytose indicator beads only), respectively.

The internalized particles usually place in the same layer of AM, whereas adhered particles do not.

After microscopic observation, cells were then harvested by cell scraper, washed by PBS, and determined by flow cytometer (FACS, BDLSR_Cell Quest Pro). The excitation wavelength is 505 nm, and the emission wavelength is 515 nm. From the plot of forward scatter against side scatter, AM was extracted (gated), and the free particles and cell-associated particles could be differentiated on the basis of size and granularity. Their mean fluorescence intensity was analyzed. The phagocytic ability was expressed using the geometric mean of fluorescent intensity of the swallowed beads from total 10 thousand extracted cells per exposure.

Cell Morphology Observed by Optical Microscopy. Cell culture morphology was routinely checked by a phase-contrast inverted microscopy at 200× magnification. Control and treated cultures were monitored both at the beginning and the end of each experimental time point.

Electron Microscopic Observation. The ultrastructural alterations of AM induced by the tested nanoparticles were observed with a transmission electron microscopy (Hitachi H-600). After a 6-h exposure, AM was harvested by a cell scraper and washed with PBS and then prefixed with 1% glutaraldehyde at 4 °C for 3 h. After being washed, AM was postfixed with 1% osmium tetroxide at 4 °C for 3 h and washed with 0.10 M cacodylate buffer. Then, cells were observed

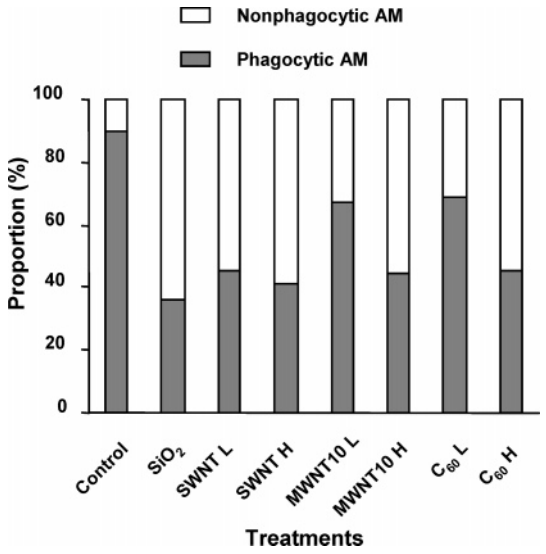

FIGURE 4. Percentage of AM capable of phagocytosing indicator latex beads after exposure to nanoparticles (defined as phagocytic AM) and unable to phagocytose the indicator latex beads after the exposure to tested nanoparticles (defined as nonphagocytic AM). The control and quartz are also presented. L represents a low dose (0.38 μg/cm^2), and H means a high dose (3.06 μg/cm^2). The dose of quartz is 3.06 μg/cm^2.

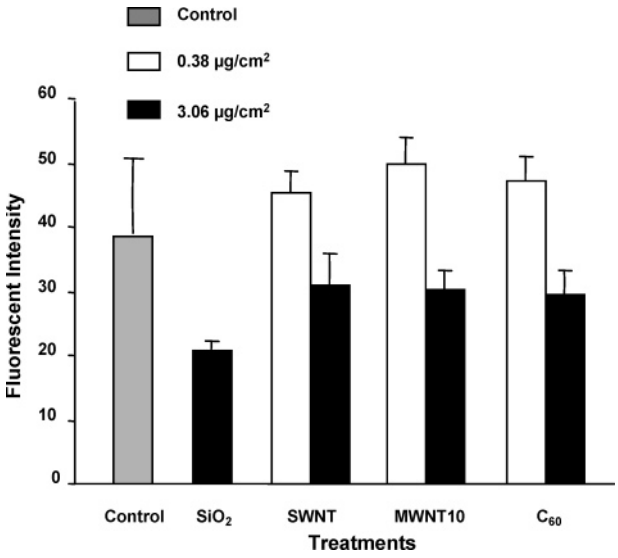

FIGURE 5. Fluorescent intensity of latex beads phagocytosed by AM exposed to SWNTs, MWNT10, C_{60}, and SiO_2. Results are the mean $\pm$ SE of triplicate experiments. $P < 0.05$.

with the TEM after dehydration, resin embedding, ultrathin sectioning, and staining with uranyl acetate and lead citrate.

Statistical Analysis. Results were calculated as the mean $\pm$ SE of the triplicate experiments. The significance of the results was statistically analyzed by a one-way analysis of variance (ANOVA) with Tukey's multiple comparison for pairwise comparison. Statistical significance was set at $P < 0.05$.

Results and Discussion

Inhalation exposure to carbon nanomaterial is currently limited to people in laboratories and related workplaces. Preliminary studies in several workplaces suggest that SWNTs are difficult to disperse as an aerosol and tend to clump into large masses (*5*). Nevertheless, inhalation of small clumps may pose problems for normal lung defenses, with the possibility of it acting as a large surface area, nonfibrous particles, or being separated into single fibers by the action of lung surfactant (*5*). Moreover, the potential similarity in size and shape between carbon nanotube and asbestos fiber has led to grave concerns about their safety.

Cytotoxicity in Terms of MTT Reduction. Figure 1 shows the cytotoxicity in terms of MTT reduction in lung AM induced by SWNTs and MWNT10 in a dose-dependent manner. Even at a very low dose level of 1.41 μg/cm^2, SWNTs show a high cytotoxicity of >20% inhibition. MWNT10 induces the significant cytotoxicity too, ~14% inhibition at 22.60 μg/cm^2. These results give some important information on the biological activities of the carbon nanomaterials studied. First, at a same dose, the cytotoxicity caused by SWNTs is much heavier than that by MWNT10. Second, at a lower dose range, the cytotoxicity of SWNTs increases much faster than that of MWNT10. This suggests that the dose-dependent manners of cytotoxicity for SWNTs and MWNT10 are different. Unlike SWNTs and MWNT10, C_{60} does not induce the observable cytotoxicity in a dose range from 1.41 to 226.00 μg/cm^2.

The results provide us with the possibility to compare the cytotoxicity between SiO_2 and SWNTs. The cytotoxicity produced by SWNTs was 61.0%, which is significantly higher than 15.7% of SiO_2 at a same dose of 22.60 μg/cm^2. This observation is compatible with result of Lam et al. (*7*) that a carbon nanotube is much more toxic than quartz in lungs. The cytotoxicity of the three types of carbon nanomaterial studied is compared in Figure 2. It reveals a sequence order of their cytotoxicity: SWNTs > MWNT10 > SiO_2 > C_{60}, at a mass basis. However, it is noted that the purity of SWNTs used in the experiment was ~90%. The impurity including mainly amorphous carbon and a trace amount of metallic catalysts, such as Fe, Ni and Y, that may somewhat influence the cytotoxicity observed. To clarify this point, the ultrapure SWNTs and MWNT10 should be employed in the further study.

Phagocytic Response after Exposure to Different Nanomaterials. Phagocytic ability is a major function of AM that largely affects the immunological potential of lungs and other related organs. Upon the fluorescent microscopic observation, we examined the phagocytic response to 2 μm latex beads after 6-h exposure to carbon nanoparticles tested to evaluate the nanomaterial-induced inhibition of the phagocytic ability of AM.

The main function of AM is to engulf the foreign material, in the present case, to engulf the carbon nanomaterial and latex beads of indicator. As shown in Figure 3, four kinds of AM are observed after MWNT10 and C_{60} treatment. (i) Cells phagocytose indicator latex beads after uptake of the tested nanoparticles (PM, in Figure 3f). (ii) Cells phagocytose the nanoparticles but are then unable to further phagocytose the indicator beads (PIP Figure 3e,g,h). (iii) Cells do not phagocytose the nanoparticles or indicator beads, suggesting that those cells are nonphagocytic after exposure to the nanoparticles (NPM, Figure 3d). (iv) Cells phagocytose only the latex beads but not the nanoparticles (PC, Figure 3g,d). But for SWNTs and quartz, by the microscopic observation it is difficult to see them inside the cells at the used magnitude of the magnification. Thus, it was quantified upon the microscopic observation by counting randomly five hundred cells per treatment, and they were divided into one of two categories: (i) Cells could phagocytose two or more indicator latex beads after exposure to the tested nanoparticles that were addressed as phagocytic AM (PM). The counts reflected the total phagocytic ability of the AM population after the exposure. (ii) Cells did not phagocytose the indicator latex beads after the exposure to the tested nanoparticles that were addressed as non-phagocytic AM (NPM). The population of each category was expressed as a percentage of the total number of AM counted.

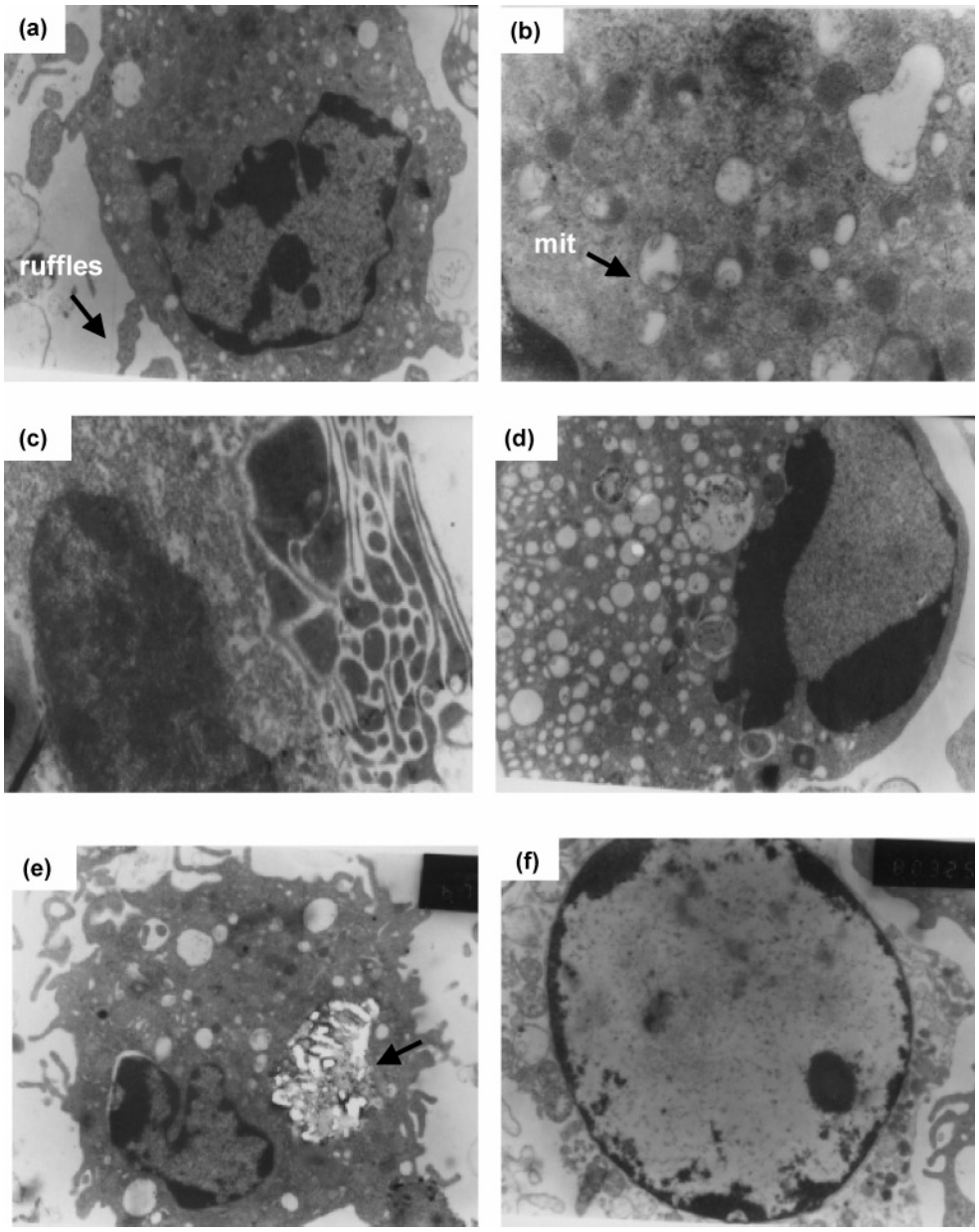

FIGURE 6. Ultrastructural changes of AM exposed to SWNTs and MWNT10 at different doses. (a and b) Cells of control at 8000× and 27000× magnification, respectively. Arrows indicated ruffle and mitochondria (mit). The cell structure is intact, and the shape of AM appears round (a). (c) Cells exposed to SWNTs of 0.38 μg/cm^2 at 10000× magnification. The condensed folds and the formation of plywood body are observed and shown by the arrow. (d) Cells exposed to SWNTs of 3.06 μg/cm^2. The swelling of the endoplasmic reticulum, vacuolar changes, phagosomes, and chromatin condensation at nuclear envelope are seen at 8000× magnification. (e) Cells exposed to MWNT10 of 0.38 μg/cm^2 at 6700× magnification. Phagosome is indicated by the arrow. (f) AM experience degeneration after exposure to MWNT10 of 3.06 μg/cm^2 at 8000× magnification.

Of great interest is the potential for SWNTs particles to impair phagocytosis more than other nanoparticles studied. SWNTs significantly impaired AM phagocytosis at a very low dose of 0.38 μg/cm^2, whereas the other test of nanoparticles achieved this effect only at a higher dose of 3.06 μg/cm^2 (Figure 4). The proportion of nonphagocytic cells was most striking in SWNTs-treated group at the lowest dose of 0.38 μg/cm^2. In fact, at all doses, SWNTs caused a larger number of AM to be nonphagocytic compared to MWNT10 and C_{60}. The results showed that, as the dose of nanoparticles increased, there was a change in the AM population from cells phagocytosing the indicator beads to cells non-phagocytosing (Figure 5). Meanwhile, the effect of SWNTs on AM phagocytosis even at a very low dose of 0.38 μg/cm^2 is nearly that of quartz at a high dose of 3.06 μg/cm^2.

Flow cytometry offers rapid, sensitive, and reproducible measurements of single cells in suspension and was employed to measure the intensity of the labeled fluorescence of latex beads phagocytosed per cell. However, the geometric mean of phagocytic latex beads detected by flow cytometer could not show an impaired phagocytic activity after exposure to the nanomaterial at a very low dose of 0.38 μg/cm^2. At a high dose of 3.06 μg/cm^2, the geometric mean of latex beads fluorescence declined to 30.85, 30.24, and 29.62 for SWNTs, MWNT10, and C_{60}, respectively, while that of the positive control (quartz) was only 20.74 (Figure 5). These results are in agreement with the fluorescent microscopic observations.

The phagocytic ability of AM obviously was reduced with the dose increase of nanoparticles. On a mass basis, SWNTs

impaired phagocytosis more than quartz or MWNT10 or C_{60}. This could be ascribed to factors including differences in geometric structures, particle number, and surface area of the tested particles. On the basis of the present results, it is inferred that during the exposure process, the nanoparticles first produce direct inhibition of the normal AM phagocytosis and are subsequently captured by and built-in AM. The laborious microscopic examination can differentiate between the bound and the ingested particles and the number of intracellular fluorescence labeled latex beads as well as the aggregates of particles, whereas flow cytometry can offer rapid measurements of single cells in suspension. Thus, these two kinds of methods can compensate each other.

Ultrastructural Alterations. Figure 6 shows the TEM images of the ultrastructural features of AM exposed to carbon nanomaterials. In the control group (Figure 6a,b), the cell structure is intact, and the shape of the macrophage appears round. A considerable number of ruffles, mitochondria, and sparse phagosomes were observed in the control cell. In cells treated by SWNTs at 0.76 $\mu g/cm^2$ (Figure 6c), the condensed folds and the formation of plywood body were observed. When the dose increases to 3.06 $\mu g/cm^2$ (Figure 6d), the swelling of the endoplasmic reticulum, vacuolar changes, and phagosomes were explicitly seen. In cells treated by 0.76 $\mu g/cm^2$ MWNT10, a large phagosome was observed (Figure 6e). When the dose increases to 3.06 $\mu g/cm^2$, the nucleus experiences degeneration, enlargement, and rarefaction of nuclear matrix (Figure 6f). Moreover, chromatin condensation at nuclear envelope, some condensed organelles and vacuolar changes in cytoplasm, and formation of surface protrusions appeared in both SWNT and MWNT10 treated groups at 3.06 $\mu g/cm^2$ that are all likely to be the consequences of the apoptotic process. Yet, additional work should be conducted to further confirm this speculated apoptotic process.

In conclusion, the tested carbon nanomaterials (SWNTs, MWNT10, and C_{60}) exhibit quite different cytotoxicity to AM. Cytotoxicity of studied nanomaterials was observed at a relatively lower dose. The cytotoxicity was indicated by the MTT reduction, loss of the phagocytic ability, and imaging ultrastructures of injured AM. The comparative toxicities of three types of carbon nanomaterials to AM are different, although they may or may not reflect in the real toxicological effects in vivo. The results suggest that human and environmental health risks of different carbon nanomaterials must be evaluated individually.

Acknowledgments

The authors are grateful to Prof. Yuanfang Liu of Peking University for his insightful advice and to Prof. Zhifang Chai of Institute of High Energy Physics for his encouragement. We acknowledge the funding supports of the major project (No. 10490180), the common project (No. 10275071) from Chinese National Natural Science Foundation, the Ministry of Science and Technology (MOST, 2001CCA3800), National Center for Nanosciences and Nanotechnology, and the Chinese Academy of Sciences. A portion of experiments described was carried out at the Beijing Synchrotron Radiation Facility.

Literature Cited

(1) Colvin, V. L. The potential environmental impact of engineered nanomaterials. *Nat. Biotechnol.* **2003**, *21*, 1160−1170.

(2) Warheit, D. B. Nanoparticles: Health impacts? *Mater. Today* **2004**, *7*, 32−35.

(3) Ball, P. Roll up for the revolution. *Nature* **2001**, *414*, 142−144.

(4) Masciangioli, T.; Zhang, W. X. Environmental technologies at the nanoscale. *Environ. Sci. Technol.* **2003**, *37*, 102A−108A.

(5) Maynard, A. D.; Baron, P. A.; Foley, M.; Shvedova, A. A.; Kisin, E. R.; Castranova, V. Exposure to carbon nanotube material: aerosol release during the handling of unrefined single-walled carbon nanotube material. *J. Toxicol. Environ. Health A* **2004**, *67*, 87−107.

(6) Warheit, D. B.; Laurence, B. R.; Reed, K. L.; Roach, D. H.; Reynolds, G. A.; Webb, T. R. Comparative pulmonary toxicity assessment of single-wall carbon nanotubes in rats. *Toxicol. Sci.* **2004**, *77*, 117−125.

(7) Lam, C. W.; James, J. T.; McCluskey, R.; Hunter, R. L. Pulmonary toxicity of single-wall carbon nanotubes in mice 7 and 90 days after intratracheal instillation. *Toxicol. Sci.* **2004**, *77*, 126−134.

(8) Dreher, K. L. Health and environmental impact of nanotechnology: toxicological assessment of manufactured nanoparticles. *Toxicol. Sci.* **2004**, *77*, 3−5.

(9) Lippmann, M. Nature of exposure to chrysotile. *Ann. Occup. Hyg.* **1994**, *38*, 459−467, 408.

(10) Shi, Z. J.; Lian, Y. F.; Zhou, X. H.; Gu, Z. N.; Zhang, Y. G.; Iijima, S.; Li, H. D.; ToYue, K.; Zhang, S. L. Production of single-wall carbon nanotubes at high pressure. *J. Phys. Chem. B* **1999**, *103*, 8698−8701.

(11) Shi, Z. J.; Lian, Y. F.; Liao, F. H.; Zhou, X. H.; Gu, Z. N.; Zhang, Y. G.; Iijima, S. Purification of single-wall carbon nanotubes. *Solid State Commun.* **1999**, *112*, 35−37.

(12) Moeller, W.; Hofer, T.; Ziesenis, A.; Karg, E.; Heyder, J. Ultrafine particles cause cytoskeletal dysfunctions in macrophages. *Toxicol. Appl. Pharmacol.* **2002**, *182*, 197−207.

(13) Mosmann, T. Rapid colorimetric assay for cellular growth and survival: application to proliferation and cytotoxicity assays. *J. Immunol. Methods* **1983**, *65*, 55−63.

Received for review August 15, 2004. Revised manuscript received December 18, 2004. Accepted December 20, 2004.

ES048729L